

Development of Software Testbed Using Parametric Design Approaches for a Series Hybrid Military Vehicle

S.J. Lee¹, J.C. Kim¹, H.S. Bae², D.H. Choi³ and B.H. Cho¹

¹ School of Electrical Engineering and Computer Science, Seoul National University

² Engineering Research Institute, Seoul National University, ³ Research Center, Defense Program, Samsung Techwin
E-mail : jun21583@snu.ac.kr

Abstract- This paper deals with the component sizing of a series hybrid electric vehicle (HEV). Since the component sizes are interrelated with the power-train structures and power control algorithm, the optimal sizing cannot be determined in a simple manner. Thus, in order to simplify the sizing problem for the HEV, this paper presents parametric design approaches which identifies the sizing effects with respect to control frequency changes of each component based on a low pass filtered power control algorithm. By using the functional simulation model with Matlab/Simulink, the proposed methods can easily and rapidly calculate the power and energy capacity of each component from the heuristic rules. The component size for designing the system is determined by a weighted cost function including the mass, volume and efficiency. This paper shows the design procedure of the proposed approaches for a 6x6 series hybrid electric armored wheeled vehicle.

I. INTRODUCTION

HEVs in military applications are being developed for better performance in survivability, maneuver and lethality. To achieve these goals, HEVs in the military require silent watch, silent mobility, fast acceleration and high gradeability for field operations [1]. Thus hybrid components including the electric motor, primary source (in this case, diesel engine and generator), energy storage element (ESE) such as battery, supercapacitor(SC), etc, should be appropriately designed considering the performance and fuel economy as well as the mission completeness.

There are several approaches for designing HEV components [2-4]. Optimization techniques, such as sequential quadratic programming and dynamic programming, are applied to the system design process and the optimal fuel consumption problem. But they suffer from taking much computation time and the power control algorithm can not be implemented in the real-time. On the other hand, heuristic methods such as the parametric design method [4] are presented to size the component capacity and to analyze effects of the component parameter variations. Although the parametric design method is not based on optimization techniques, it makes problems simple by determining the component capacity from the power and energy equations within given constraints. And it has advantages of giving the concept and direction for the component sizing problem. But

the effects of the power control algorithm implemented to the system should be analyzed in detail.

Thus, this paper presents parametric design approaches which identify the sizing effects with respect to control frequency changes of each component based on a low pass filtered power control algorithm. The design procedures are as follows: first, the rating of the electric motor is designed from the required performance constraints such as acceleration and gradeability. Then, the power and energy capacity of the primary source (diesel engine) and the electric energy storages are determined from the simulated results with respect to the filter cutoff frequency changes of the power control algorithm. Among the collected results, the power and energy ratings of each component are determined by a weighted cost function including the vehicle mass, volume and the efficiency.

A design example of a 6x6 series hybrid electric armored wheeled vehicle is given to show the procedure of the proposed design sequence.

II. SYSTEM AND COMPONENT MODELING

A. System Architecture of SHEV

The simplified system architecture of a 6x6 armored wheeled vehicle is shown in Fig. 1. As a series hybrid electric vehicle (SHEV), the diesel engine is the primary power source and the electric energy storage system (ESS) consisted of a battery and SC with bi-directional DC-DC converters is the secondary power and energy source. Also for the propulsion of the vehicle, the in-wheel motor in each wheel is applied to the system for achieving better mobility and reducing the system space. Thus the main components, such as the engine, battery, SC and electric motor should be appropriately designed to achieve satisfactory and stable vehicle operation in addition to better fuel economy [5, 6].

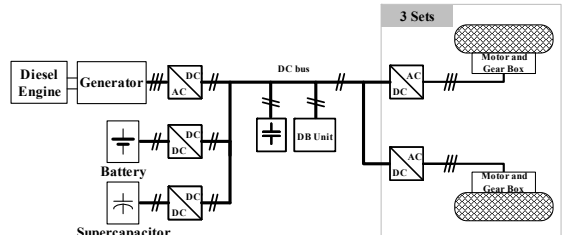


Fig. 1. System architecture of series hybrid electric wheeled vehicle

B. Engine Model

To model the diesel engine, the steady state variables, such as the engine torque, speed and fuel rate are necessary in the functional simulation model. Thus, the engine is modeled using a characteristic map obtained from experimental results. In this work, two characteristic maps have been used. One is the engine torque map of Fig. 2 which has inputs of the engine speed and throttle position. The other is the fuel consumption map of Fig. 3 which has inputs of the engine speed and torque. And then, the engine speed is calculated by the motion equation using the generated engine torque and the controlled generator torque. For the base characteristics of the engine, the Detroit Diesel Corp. Series 30 7.3L diesel engine [7] was used and the scaling of the engine is adjusted by a linear factor.

C. Motor and Generator Model

Because the model parameters are unknown in the designing phase, we used the motor capability curve which represents the steady state characteristics related with the motor speed and torque as shown in Fig 4. The available output torque transferred to the wheels or gears at a given input torque reference is modeled into a simulation model block in Matlab / Simulink.

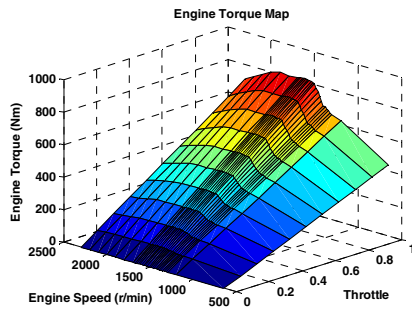


Fig. 2. Engine characteristic map

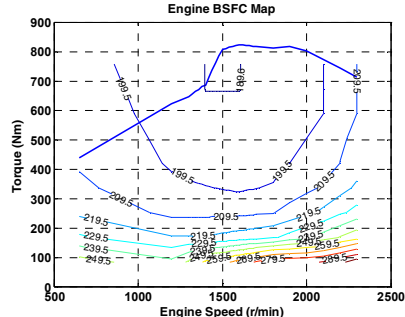


Fig. 3. Engine fuel consumption map

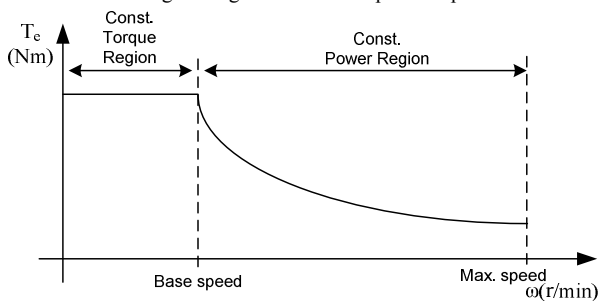


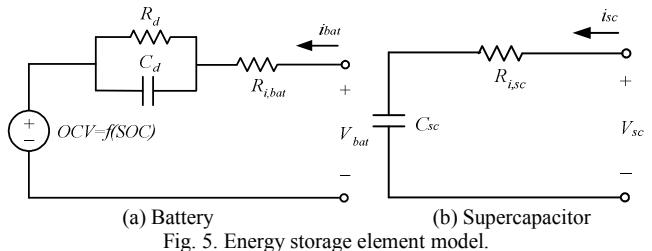
Fig. 4. Motor capability curve

D. Electric Energy Storage Model

The energy storage element (ESE) models, in this case the battery and the SC, are built based on the equivalent electrical circuits. The equivalent circuit model of a Li-polymer battery consists of an internal voltage source equivalent to the open circuit voltage (OCV), a series resistance of $R_{i,bat}$ and a parallel connection of R_d and C_d as shown in Fig. 5 (a). Likewise, the SC has an equivalent circuit consisted of an ideal capacitance of C_{sc} and a series resistance $R_{i,sc}$ as shown in Fig 5 (b). Fig 6 shows the open circuit voltage versus state of charge (SOC) of a 14Ah nominal capacity Li-polymer cell. The parameters of the ESE are tabulated in Table I. Although these vary according to the temperature, energy level and current magnitude, parameters in the nominal condition are sufficient in the designing phase.

E. Vehicle Dynamics Model

For the component sizing, we only consider the longitudinal dynamics for a given vehicle velocity that is called to the driving cycle. Thus the vehicle is modeled using the combined relationship of the wheel angular motion and the longitudinal motion of the vehicle is related to the tractive force of the motor, $F_{tractive}$, and the road load such as the rolling resistance of F_{roll} , aerodynamic resistance of F_{air} and grade resistance of F_{grade} . These are represented as (3)-(5).



(a) Battery (b) Supercapacitor
Fig. 5. Energy storage element model.

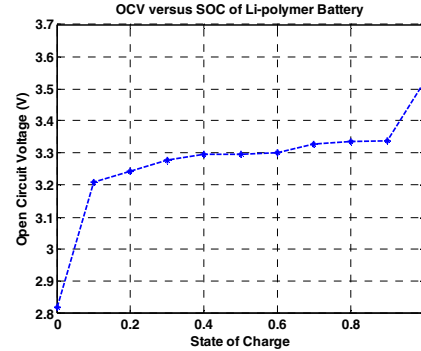


Fig. 6. Open circuit voltage versus state of charge of Li-polymer cell

TABLE I
PARAMETERS OF ENERGY STORAGE ELEMENT

Type	Parameters			
	R_i ($m\Omega$)	R_d ($m\Omega$)	C_d (F)	C_{sc} (F)
Li-polymer cell	1.35	2.6	3850	.
Supercapacitor cell	0.4	.	.	5000

$$Ma = F_{tractive} - F_{roll} - F_{air} - F_{grade} \quad (1)$$

$$J_w \frac{d\omega_w}{dt} = T_w - T_b - rF_{tractive} \quad (2)$$

$$F_{roll} = f_r \times M g \cos(\theta) \quad (3)$$

$$F_{air} = \frac{1}{2} \rho C_d A_f v^2 \quad (4)$$

$$F_{grade} = M g \sin(\theta) \quad (5)$$

where, M is the vehicle mass, a is the acceleration of the vehicle, ω_w is the angular speed of the wheel, J_w is the moment of the inertia of the wheel, T_w is the wheel torque from the motor and gear, T_b is the frictional braking torque, r is the effective wheel radius, f_r is the rolling resistance coefficient, g is the gravity acceleration coefficient, θ is the road slope, ρ is the air density, C_d is the aerodynamic coefficient, and A_f is the frontal area of the vehicle.

F. Overall System Model

For application of the proposed method, fast simulation and ease in implementing the algorithm are required. Thus the overall functional vehicle model is built with in the Matlab /Simulink environment using the backward-facing approach [8]. The simplified block diagram for the simulation is shown in Fig. 7.

III. COMPONENT SIZING OF HYBRID ELECTRIC VEHICLE

The HEVs should be designed to meet the required driving performances and to minimize the vehicle weight for the fuel economy in the given system parameters. In addition to these, the system has also a volume constraint. Thus the system is designed to minimize the weighted cost function [9] which is defined by the system mass, volume and efficiency related to each maximum constraint value as (6).

$$f = \alpha_M \frac{M}{M_{max}} + \alpha_V \frac{Vol}{Vol_{max}} + \alpha_\eta (1 - \eta_{eff}) \quad (6)$$

where, M_{max} is the vehicle maximum mass, Vol_{max} is the maximum volume of the hybrid component (engine, generator, battery, SC, motors and power conversion devices), η_{eff} is the ratio of the consumed energy for the propulsion to the consumed energy from the engine, and α_M , α_V and α_η are the weighting factors whose sum equals one.

In this work, a design example of a 6x6 all wheel driven vehicle is given, and the system parameters and the performance constraints are tabulated in Table II - III. Thus,

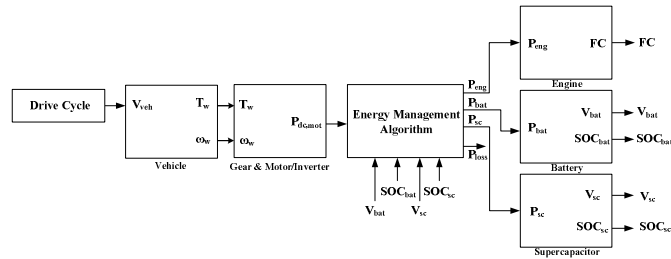


Fig. 7. Block diagram of the backward-facing simulation model

TABLE II
SYSTEM PARAMETERS

Parameter	Value	Parameter	Value
Gross Vehicle Weight	10,000 kg	Frontal Area	4.5 m ²
Wheel radius	0.5 m	Aerodynamic Coefficient	1
Rolling resistance	0.01 + 0.001×V(km/h)		

TABLE III
PERFORMANCE CONSTRAINTS

Acceleration	0 – 48 km/h at 8 seconds
Max. speed	110 km/h
Gradeability	10 km/h at 60% slope

the main components, such as the electric motor, battery, SC and the engine, for a SHEV are sized as follows.

A. Electric Motor Sizing

The electric motor is the only propulsion device in a SHEV and should be appropriately designed to satisfy the demanded torque and speed of the load. The power for acceleration and cruising speed can be derived based on the Second Law of Newton as (7)-(8) [4, 10].

$$P_{tr} = \frac{M_{eq}}{2t_a} (v_f^2 + v_b^2) + \frac{2}{3} Mg f_r v_f + \frac{1}{5} \rho C_d A_f v_f^3 \quad (7)$$

$$P_{tr,cr} = (Mg(f_{r,init} + f_{r,inc} v_{cr}) + 0.5 \rho C_d A_f v_{cr}^2) v_{cr} \quad (8)$$

where, t_a is the required acceleration time, M_{eq} is the equivalent vehicle mass including inertia, v_f is the final speed of acceleration, v_b is the vehicle speed corresponding to the motor base speed, $P_{tr,cr}$ is the demanded power at cruising speed, and v_{cr} is the cruising speed of the vehicle.

In military applications, because the performance constraint for the gradeability is more severe than commercial vehicles, the maximum torque of the motor should be carefully sized. In the case of all wheel driven vehicles, the maximum torque of the motor can be calculated from the maximum tractive force related to the normal load of each wheel on an inclined road [11]. Also, in order to reduce the power and torque rating of the motor, the gear ratio and the constant power speed ratio (CPSR) should be appropriately selected depending on the motor type [4]. Fig. 8 shows the maximum rating of each motor sized for satisfying the given constraints, where the gear ratio is 10.

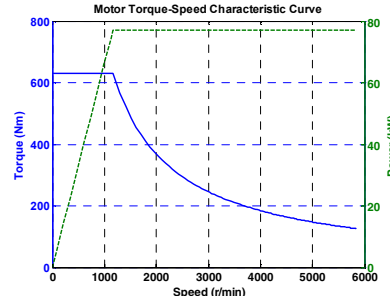


Fig. 8. Motor torque-speed characteristic curve

B. Primary and Secondary Source Sizing

The diesel engine-generator is the primary power source in this example, and it supplies the average power during the driving cycle and assists the required peak power during acceleration, and also when needed at peak road load demand. On the other hand, the secondary source, which is comprised of the battery and the SC, has the ability to assist the engine and to regenerate the braking energy. Especially, the battery should be able to supply sufficient power and energy during silent operations in military applications. In order to design the components, the inequalities of the power and energy requirements can be derived from several constraints.

Since the diesel engine is required to supply an average amount of power during the driving cycle, equation (8) and inequality (9) can be formulated.

$$P_{eng} \geq \frac{1}{\eta_{engen}\eta_{gen}} \left(\frac{P_{tr,cr}}{\eta_{mot}\eta_{gr}} + P_{aux} - \frac{P_{bat,ch}}{\eta_{bdc}\eta_{bat}} \right) \quad (9)$$

where, P_{aux} is the auxiliary load power including air-conditioning, $P_{bat,ch}$ is the battery charging power, and η_{engen} , η_{gen} , η_{mot} , η_{gr} , η_{bdc} and η_{bat} are the engine-generator coupling, generator, motor, gear, DC-DC converter and battery efficiencies respectively.

The constraints for the battery and SC are represented as (10)-(13). Due to the power and energy balance, both should be able to assist the engine power on a given road load and have sufficient energy for the driving cycle and silent operations. From (10), the sizing of the primary and secondary sources are interrelated with each other and depends on the power distribution method. Thus, a low pass filtered power control algorithm is applied as shown in Fig. 9. This is a heuristic method where the engine supplies the average load power and the ESS supplies the peak power, and regenerates the braking energy. When considering the efficiency of the battery, SC and bi-directional converters, this means that the steady power of the load comes from the primary power source. The applicability of the power control algorithm is validated in Section IV.

$$P_{bat} + P_{sc} \geq \frac{P_{tr,max}}{\eta_{bat}\eta_{bdc}\eta_{mot}\eta_{gr}} - \frac{P_{eng}\eta_{gen}\eta_{engen}}{\eta_{bat}\eta_{bdc}} \quad (10)$$

$$E_{bat} + E_{sc} \geq \max\{E_{ev}, E_{driving}\} \quad (11)$$

$$E_{bat,min} \leq E_{bat} \leq E_{bat,max} \quad (12)$$

$$E_{sc,min} \leq E_{sc} \leq E_{sc,max} \quad (13)$$

where, P_{bat} is the desired discharging power rating, P_{sc} is the maximum SC power rating, $P_{tr,max}$ is the maximum traction

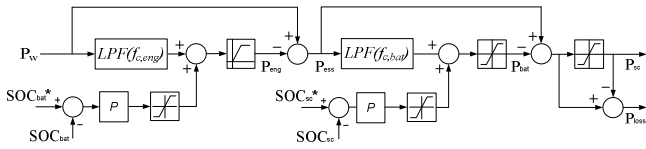


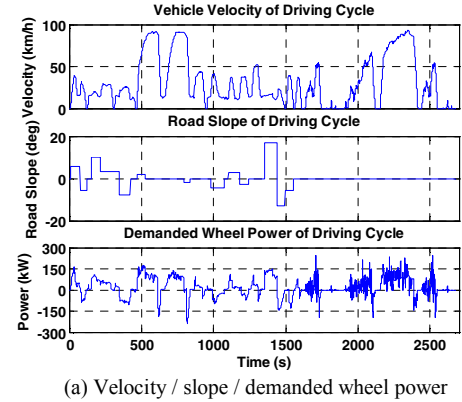
Fig. 9. Low pass filtered power control algorithm

power, E_{bat} is the desired battery energy capacity, E_{sc} is the SC energy capacity, E_{ev} is the demanded energy for silent operation, $E_{driving}$ is the demanded energy during the driving cycle, $E_{bat,min}$ and $E_{sc,min}$ are the specified minimum energy of the battery and SC, and $E_{bat,max}$ and $E_{sc,max}$ are the specified maximum energy of the battery and SC.

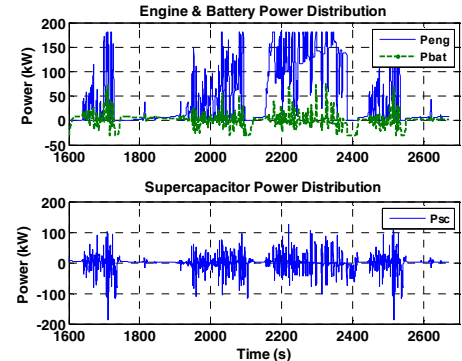
IV. SIMULATION RESULTS

The simulation is carried out to find the component sizing using the proposed method. The main procedures of designing the powertrain components are as follows. First, the initial vehicle parameters and performance constraints are inputted into the program. Next, the electric motor is sized from the vehicle specifications and the performance constraints. Thirdly, according to the power control algorithm and the cutoff frequency changes of the low pass filter, denoted to LPF in Fig. 9, the power and energy capacity of the battery and SC are determined to satisfy the demanded power for drive cycle, and the power ratings of the power conversion devices such as the bi-directional DC-DC converters for the battery and SC, inverters for traction motors, and the AC-DC converter for the generator are designed. Thus, according to the determined power and energy rating of each component, the gross vehicle weight (GVW) is calculated by the specific power and energy, and the power and energy density of each component.

Fig. 10 shows the simulation results of the proposed method. Because the driving pattern for the military



(a) Velocity / slope / demanded wheel power



(b) Engine / battery / SC power distribution during 1600-2700 seconds

Fig. 10. Simulation results over the mixed drive cycle

application is not known, the driving cycle mixed with the tactical operation cycles (which is intentionally made in this work) and the hd-udds [12] (which is the typical driving cycle for the heavy duty vehicle) has been applied to the simulation. In Fig. 10 (b), since the power distribution of the demanded wheel power during the driving cycle is performed by the proposed power control algorithm, the required power and energy ratings of the battery and SC can be determined.

Fig. 11 shows the comparison results of the proposed power control algorithm (denoted to RB in Fig. 11) and the optimal power distribution for minimizing the consumed engine energy using linear programming (LP) [13] during the 0-1060 seconds. The linear programming method is formulated with the power and energy balance equation, and the slew rate constraints of the power variation of the engine and battery similar as [14]. From the solid line of Fig. 11, in order to maximize the system efficiency, the diesel engine should supply the steady power of a road load and an auxiliary load including the cooling system. Because LP uses future information such as the grade and speed, the power distribution results are a little different between LP and the proposed power control method which are represented as dotted line in Fig. 11. But similar power distribution from a real-time controller can be achieved and the results obtained from variation of the cutoff frequency of the power control algorithm are applicable to design the system.

Fig. 12 shows the sizing results with respect to the cutoff frequency changes of the low pass filter of the power control method. The electric motor is previously designed in Section III and the diesel engine is chosen to supply the demanded power for the maximum vehicle speed. At this time, from the weighted cost function of Fig. 12 (f), the region A is chosen. Thus the power capacity of the battery and SC can be determined from Fig. 12 (a)-(b) and the energy capacities can also be determined through the same procedures even if not shown in the figures.

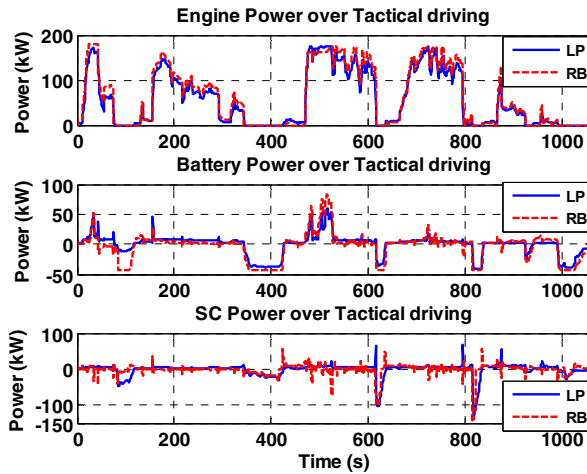
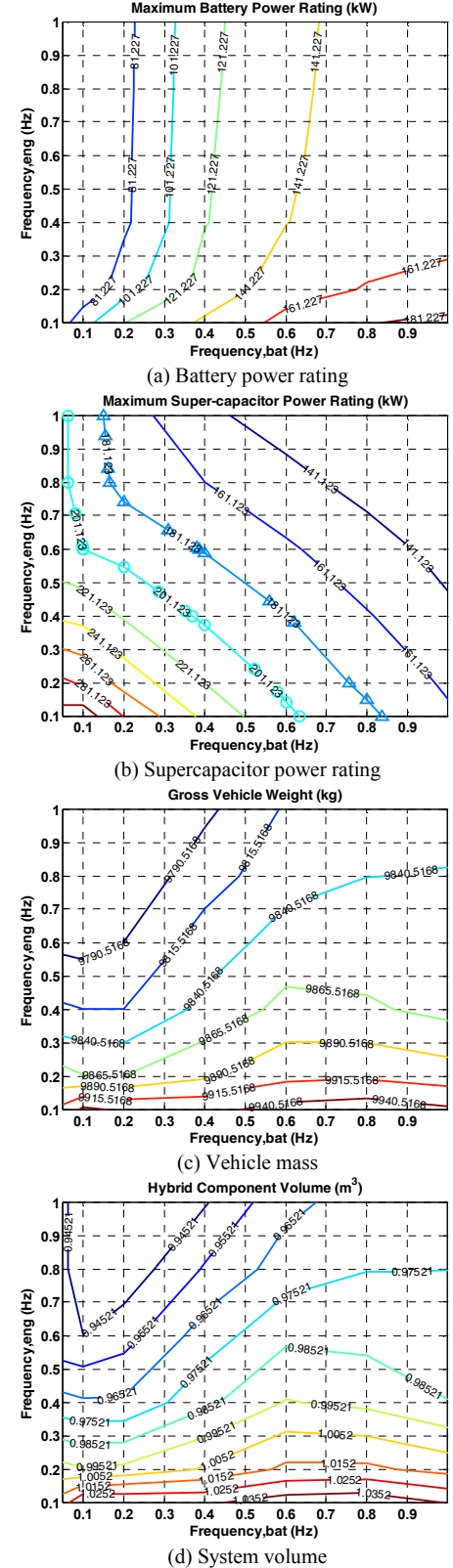


Fig. 11. Power distribution comparison between LP and proposed method.



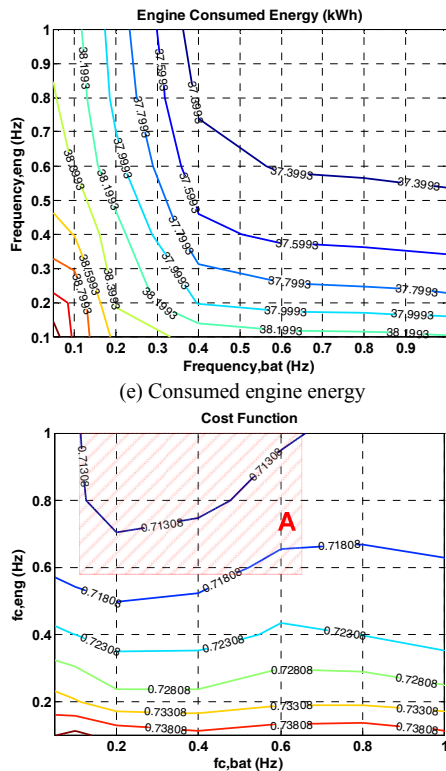


Fig. 12. Component sizing distribution with respect to the control bandwidth changes at 180 kW engine power.

V. CONCLUSION

This paper introduces the methodology of sizing the HEV components using a heuristic method based on a low pass filtered power control algorithm. When given vehicle parameters and performance specifications, the electric motor is designed to meet the performance constraints such as acceleration and gradeability. And the diesel engine and the ESS are determined to minimize the weighted cost function including the total vehicle mass, volume and efficiency. A 6x6 series hybrid electric armored wheeled vehicle is given as an example to show the design procedure in detail.

ACKNOWLEDGMENT

This work was supported by Research Center, Defense Program of Samsung Techwin.

REFERENCES

- [1] G. Khalil and Jennifer Hitchcock, "Ground Vehicle Mobility Requirements. Meeting the Challenge with Electric Drives," Gas Turbine Engine Combustion, Emissions and Alternative Fuels, pp. 1–13, Jan. 1999.
- [2] E. Vinot, R. Trigui, B. Jeanneret, J. Scordia, F. Badin, "HEVs Comparison and Components Sizing Using Dynamic Programming," VPPC 2007, pp. 314-321, Sept. 2007.
- [3] M. Jain, C. Desai, S.S. Williamson, "Genetic algorithm based optimal powertrain component sizing and control strategy design for a fuel cell hybrid electric bus," VPPC 2009, pp. 980-985, Sept. 2009.
- [4] Yimin Gao and Mehrdad Ehsani, "Parametric Design of the Traction Motor and Energy Storage for Series Hybrid Off-Road and Military Vehicles," IEEE Trans. on Power Electronics, Vol. 21, No. 3, pp. 749-755, May 2006.
- [5] B.H. Lee, D.H. Shin, H.S. Song, H. Heo, H.J. Kim, "Development of an Advanced Hybrid Energy Storage System for Hybrid Electric Vehicles," Journal of Power Electronics Vol. 9. No. 1, pp. 51-60, Jan. 2009.
- [6] S. Pay, Y. Banhzouz, "Effectiveness of Battery-Supercapacitor Combination in Electric Vehicles," Proc. of Power Technology Conference, June 2003.
- [7] Advisor 2002 software, <http://www.ctts.nrel.gov/analysis>
- [8] K. B. Wipke, M. R. Cuddy, and S. D. Burch, "ADVISOR 2.1: A User-Friendly Advanced Powertrain Simulation Using a Combined Backward/Forward Approach," IEEE Trans. on Vehicular Technology, Vol. 48, No. 6, pp. 1751-1761, Nov. 1999.
- [9] T. Hofman, D. Hoekstra, R.M. van Druten, and M. Steinbuch, "Optimal design of energy storage systems for hybrid vehicle drivetrains," VPPC 2005, pp. 73-77, Sept. 2005.
- [10] M. Ehsani, Y. Gao, S. E. Gay, and A. Emadi, *Modern Electric, Hybrid Electric, and Fuel Cell Vehicles: Fundamental, Theory, and Design*, CRC Press, 2005.
- [11] Rao V. Dukkipati, Jian Pang, Mohamad S. Qatu, Gang Sheng, and Zuo Shuguang, *Road Vehicle Dynamics*, SAE, 2008.
- [12] EPA Urban Dynamometer Driving Schedule (UDDS) for Heavy-Duty Vehicles, <http://www.dieselnet.com/standards/cycles/udds.php>
- [13] P. Venkataraman, *Applied Optimization with Matlab Programming*, Wiley, 2002.
- [14] E.D. Tate and S.P. Boyd, "Finding Ultimate Limit of Performance for Hybrid Electric Vehicles," SAE Technical paper 2000-01-3099, 2000.